© Universiti Tun Hussein Onn Malaysia Publisher's Office

JAITA

http://publisher.uthm.edu.my/ojs/index.php/jaita

e-ISSN : 2716-7097

Journal of Advanced Industrial Technology and Application

Compact Real-Time Control System for Autonomous Vehicle

F. Choong[1], Leong Rong Fei[1]

[1]Heriot-Watt University Malaysia,
1, Jalan Venna P5/2, Precinct 5, 62200, Putrajaya, MALAYSIA

*Corresponding Author

DOI: https://doi.org/10.30880/jaita.2022.03.02.006
Received 15 September 2022; Accepted 6 Novemebr 2022; Available online 9 December 2022

Abstract: Due to global warming, there is an increase in the number of natural disasters occurring around the world. With more disasters happening, post disaster search and rescue personnel are putting their life on the line more often in scouting out the post disaster site and sending in first aid supplies while waiting for rescue vehicles like fire trucks and ambulance to arrive. In Malaysia alone, the use of compact Autonomous Landed Vehicle (ALV) for this purpose is limited. There are many compact ALV that are being developed with microcontrollers and microprocessors such as Arduino and Raspberry Pi as the central control system, but they are fragile and can be damaged easily when used in harsh environments. In addition, multiple microcontrollers and microprocessors are needed for the ALV as parallel processing and limited gates are some of the common problems with microprocessors and microcontrollers. In this paper, a central control system using an FPGA is proposed together with the design of a prototype for the ALV. The ALV consists of three systems: Propulsion System, Sensor System, and Remote-Control System. These systems are integrated together with the Altera DE-115 board as the central control unit of the ALV. Verilog Hardware Description language (Verilog HDL) is used for designing the control system for the ALV. The proposed system is stable, low cost, allows parallel processing and the compact size of the ALV allows smooth manoeuvring through small areas of post disaster sites to scout out the area and send in first aid supplies to the victims.

Keywords: FPGA, compact real time autonomous vehicle, Verilog HDL, Altera DE2-115, Autonomous Landed Vehicle

1. Introduction

Semi-autonomous vehicle is a vehicle that can navigate through a remote control as well as self-navigating using an intelligent navigation system [1]. The navigation system takes inputs from multiple sensors, processes the inputs obtained, then makes necessary manoeuvres required to avoid collisions. When there are scenarios that the navigation system is unable to determine the necessary course of action, the vehicle can also be controlled by an operator from a distance. The semi-autonomous vehicle has several potential applications ranging from search and rescue missions to military usage. In the past decade, many countries have been focusing on the threats of global warming towards human life. Due to global warming, the occurrence of natural disasters such as typhoon, storms, flash floods, etc. have been on the rise. A study was done on monitoring the global warming index and the results obtained of human-induced warming to the globe is at about +0.16 °C per decade [2]. These disasters pose a great challenge to search and rescue teams to react during or after the disasters. Some of these challenges include narrow and unstable pathways which would endanger the rescuers. With the compact semi-autonomous vehicle, rescuers can easily identify location of the victims and the condition of the environment where the victim is located without endangering the life of the rescuers.

The design of a compact real-time autonomous vehicle involves several factors such as power supply, path planning, weight limitation, size limitation etc. [3] A compact design for an autonomous amphibious vehicle was proposed with direct differential directional drive that has zero-radius steering [4]. The design used a field

*Corresponding author: f.choong@hw.ac.uk

programmable gate array (FPGA) as the control platform for the compact autonomous amphibious vehicle. The design has two main inputs, which are the sensor processed input and remote-controlled input. It operates on a wheel-based propulsion system which consists of 2 wheels that are connected to a DC motor. The steering system is based on the two wheels in the propulsion system with the aid of a third wheel connected to a servo motor for zero radius steering. The turning of the vehicle is achieved by varying the speed between the two wheels connected to the dc motor and the direction of which the third wheel is facing. The constrain in this design is that the wheel velocity and torque is distributed by the inherently unstable motion.

Another work proposed a compact real time control system of a four-wheeled autonomous vehicle using Altera DE1 Board [5]. The proposed design uses two wheels at the back as the propulsion system and the front two wheels for the navigation system. The dc motors are controlled by PWM pulse generated using the Altera DE1. There is a stereo camera connected to the vehicle that provides image feedback for the user and there are ultrasonic sensors as range finders.

De Castro et al. (2009) proposed an electric vehicle using a simple EC3S1000 FPGA as the control system for two motors. The design consisted of five modules which is the motor controller, the ThrottleMap, the electronic protection, the Global Manager and the Auxiliary Modules, which are additional modules to make the interface with external peripherals, such as counting pulses for the encoder, SPI communications, input debouncing etc. [6].

Afaq *et al.* (2015) proposed a design for a customizable FPGA based system for a control algorithm on an Unmanned Ground Vehicle and its 5 Degree of Freedom (DOF) manipulator. The vehicle is made of steel and aluminium plates, differential wheeled robot. This enables the vehicle to climb up steep slopes and move on rocky terrains and hilly areas. The control unit is developed using the Compact RIO-9012. An open loop control was designed whereby a human control the movement of the vehicle via a wireless joystick. Video feedback is also present from a camera installed on the vehicle. This enabled the operator to control the vehicle even when it is out of sight of the operator [7].

In a related work, a design for an obstacle avoiding robot using infrared sensors was proposed [8]. The robot design proposed by the consists of two parts, the mechanical design and the circuit design. For the mechanical design, the author uses two gear motors and wheels for the movement of the robot towards four directions: forward, backward, left, and right. To aid the free movement of the robot, a freewheeling ball is installed at the front of the robot. For the circuit design, there are two parts in the system: the sensor part and the control board. The sensor part is made out of a variable IR generator using NE555 IC generating infrared signal and variable resistors, and an IR detector. For the control board, the author uses an ATMEL 89C205I microcontroller and a motor driver L293D.

Ching-Heng Ku *et al.* (2001) proposed an obstacle detection method for a vision-based ALV through human guidance. The ALV uses a camera to detect and identify the presence of a human through image processing. Once a human is detected, the ALV will then follow the detected human through an obstacle free pathway to avoid any collision. The author mentioned some advantages on this detection method such as the discrimination of the location of the person and the obstacle, increased precision through the derived quadratic path, matching the kinematics of the vehicle *etc.* The operational process of the system starts by acquiring images from the camera, estimating the location of the vehicle, obstacle detection, prediction and detection of the human location, generating patterns between human detection and obstacle detection, path calculation, and then vehicle control [9].

Cui Huihai *et al.* (2011) proposed an obstacle detection algorithm through sonar data modelling. The author mentioned that localisation of objects is difficult for a single sensor due to the low angular resolution of the sonar, the author uses a dual sonar array, with the assumption of zero loss of the generalisation and that only the obstacles that lie within the coverage area of the two-sonar sensor will be considered. The sonar returns are then collected and compiled into an obstacle map and then accumulated into a global map. Then, the line features in the image space is then directly chosen into a parameterized space through a general sonar signal Hough transformation to improve the efficiency of the algorithm. The obstacle detection method was then testing out and the results shown that the accuracy of the distance and direction of the obstacle was high with minimal specular reflection, cross-talk, and environmental noise [10].

Tao Wu *et al.* (2017) proposed a new obstacle detection method using feature matching and fusion-based algorithm with LiDAR. Firstly, the author proposed a new method for set up for the LiDAR sensor from the conventional setup. The LiDAR sensor is tilted at the sides of the vehicle, rather than putting it up straight on top of the vehicle, with both of them angled equally forward. There were some precautions are taken, such as making sure that the LiDAR laser does not directly pointed at each other to prevent damaging the sensor. With the two LiDAR sensor tilted forward at the same angle, the coverage area of both the sensors overlaps, giving a denser range of interest hence improving the resolution of the LiDAR detection. With the information given by the LiDAR sensor, a feature matching and fusion algorithm is then used to identify the obstacles. The feature matching enables the algorithm to detected potential obstacles by comparing the features between the real scan lines from the LiDAR and the scan line that is simulated. The feature fusion combines all the features from all the LiDAR to improve the ability of obstacle detection. The results from this setup were proven to be stable and that the computational time was reduced compared to other algorithms [11].

Yongquan Xia *et al.* (2009) proposed an obstacle detection method using stereo pair matching algorithm. The method proposed does not require any sophisticated computing and image processing. The first step in the obstacle

detection is to binarize the image with a new binarization method in the proposed algorithm. All the pixels are divided into sets, one which includes the characteristic sets containing contour and edge pixels, and the other are pixels in smooth regions. The characteristic sets and the smooth region set are then binarized, with one as 1 and the other as 0. After that, the binarized images are then inner filled to avoid over segmentation. Lastly, the pair of images that are captured and processed are then matched together. Regions that are matched successfully between the two images are then considered as potential obstacles for the vehicle [12].

Karthikeyan *et al.* (2014) proposed a design for an intelligent exploration and surveillance robot. The author categorized the system operation into three parts, acquiring knowledge, allocation of task, and the interaction between devices of the robot. The author mentioned that some of the advantages in the proposed design is the motors of the robot can be controlled automatically through autonomous robot control and the surveillance system through the usage of GPS. The device also has a self-destruction system to enhance the security level of the robot. The proposed robot uses and ARM11 processor as the control unit of the robot. Several modules are present in the robot such as a MIC for audio input, camera for image input, ultrasonic sensors for distance measurement, DC motors for movement control, LDR for luminance, GPS for tracking, and a self-destruction unit. With the aid of the different modules, the author created a closed looped surveillance algorithm to analyse the various inputs from the modules [13].

In this paper, an improved design of a central control system using an FPGA is proposed together with the design of a prototype for the ALV. The ALV consists of three systems: Propulsion System, Sensor System, and Remote-Control System. These systems are integrated together with the Altera DE-115 board as the central control unit of the ALV. The proposed system is stable, allows parallel processing, low cost and the compact size of the ALV allows smooth manoeuvring through small areas of post disaster sites to scout out the area and send in first aid supplies to the victims. The reduced size of the proposed ALV enables the post disaster search operations to be carried out at lower risks and at a faster pace to increase the safety of the rescuers and the survival rate of the victims.

2. Methodology

As shown in fig. 1, the proposed ALV consists of three main parts: the propulsion system, the remote-control system and the sensor system that will run simultaneously on the Cyclone IV EP4C115F29 chip that is present on the Altera DE2-115 Board.

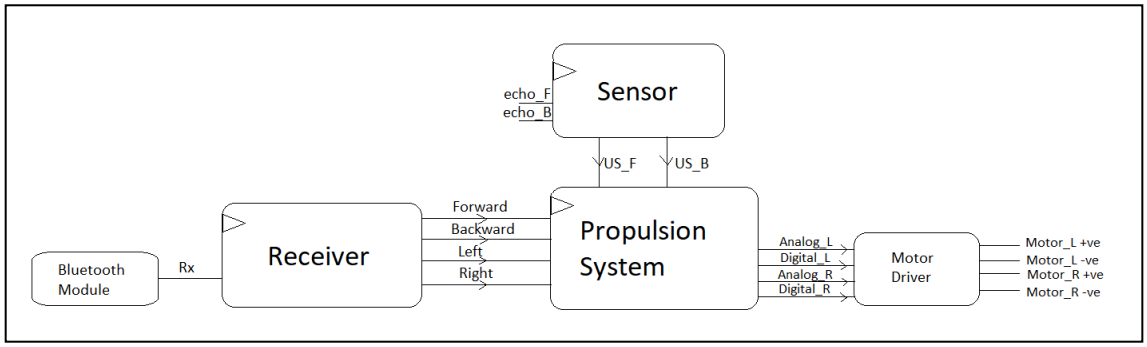

Fig. 1 - Proposed ALV system

The propulsion system consists of the Altera DE2-115 Board, SmartDriveDuo-30 motor driver, and two DC brushed motor. The system takes in six digital inputs and generates four outputs to the motor driver, two analogue outputs and two digital outputs. The motor driver then takes in the four outputs by the DE2-115 and produces the required voltages to control the DC brushed motor to rotate at the required speed and direction. The digital inputs are received from the two other systems, four from the remote-control system which indicates the movement of the ALV, and two from the sensor system which provides the collision warning for the vehicle.

The analogue output that is provided by the DE2-115 to the motor driver is a PWM signal. The rotational speed of the DC brushed motor is controlled by the duty cycle of the generated PWM, whereby 0% is the stop signal and 100% is full speed rotation. The digital outputs by the DE2-115 determines the rotational direction of the DC brushed motor whereby a HIGH pulse indicates forward rotation, and a LOW pulse indicates a backward rotation. Fig. 2 shows the state diagram of the propulsion system.

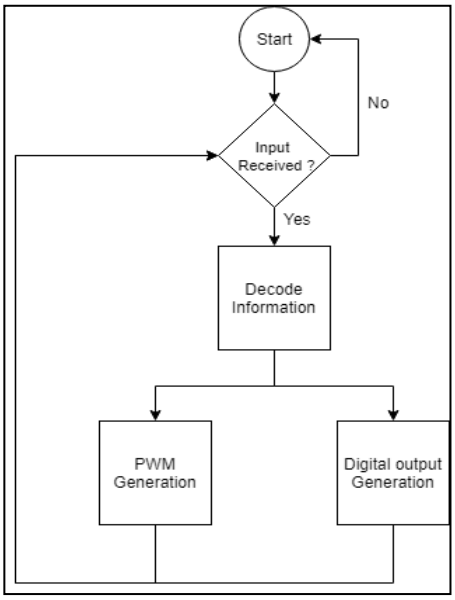

Fig. 2 - State diagram of propulsion system

The propulsion system is implemented using counters, multiplexers and decoders as shown in Fig. 3. Step down counters is used to reduce the 50 MHz clock of the DE2-115 board to a lower frequency clock for the other counters. The period counter acts as the reset signal for the duty cycle counter, indicating a new cycle for the PWM signal. The duty cycle counter controls the output of the 2-bit multiplexer, determining the output to be either a HIGH or LOW. The decoder breaks down the input signal from the remote-control system and the sensor system and then sends the information on the width of the PWM signal to the duty cycle counter.

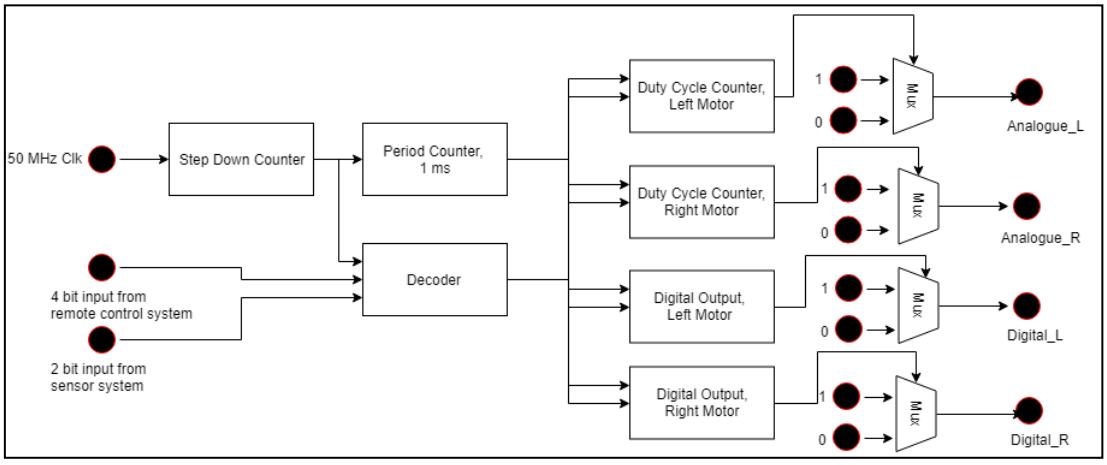

Fig. 3 - Block diagram of propulsion system

The stepdown counter, period counter, and duty cycle counters are implemented using a simple incrementor and a comparator. The base value of the comparator for the stepdown counter and the period counter is calculated through the Equation (1):

$$Base\ value = \frac{1}{Period\ of\ clock} \quad (1)$$

The base value of the comparator of the duty cycle counter is dependent on the output given by the decoder. The comparator will output a LOW signal whenever the input from the incrementor is lesser than the base value. The incrementor will increment by 1 and feeds the latest value to the comparator at every single clock cycle. When the input of the incrementor is equal to the base value of the comparator, the comparator will output a HIGH signal and the incrementor value will be reset to 0 and the process will be repeated. The decoder takes in all the inputs from the remote-control system and the sensor system and arranges it into 6 bits. The decoder then determines the base value for the duty cycle counter at various conditions. The base values for the duty cycle counter is preset into registers.

2.1 Remote-Control System

The remote-control system is implemented using Altera DE2-115 board, HC-06 Bluetooth module, and a phone with Arduino Bluetooth RC Car application installed. The system takes in the input sent by the phone to the Bluetooth module through serial communication. The DE2-115 then decodes the serial data received, decodes the signal, and then gives out a 4-bit digital output to the propulsion system.

Fig. 4 shows the design for the state machine of the remote-control system. The system has two states: Idle State and Read State. During the idle state, all parameters of the counters and counter enables are all set reset to zero. Once the start bit, which is a LOW signal, is detected from the Rx value of the Bluetooth module, the state will then change from idle state to read state. In the read state, the counters, shift registers, and data registers will start operating. When all the data is done, the state will then revert to idle state and wait for the next start bit to be detected.

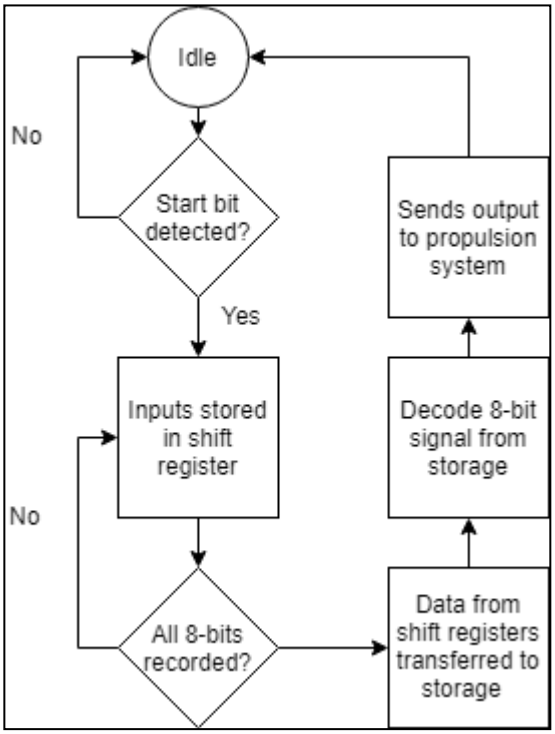

Fig. 4 - State diagram of remote-control system

Fig. 5 shows the block diagram for the remote-control system comprising counters, a register, a shift register, and a decoder. The baud rate counter takes in the 50 MHz clock and steps it down to 16 times of the baud rate of the Bluetooth module, which is 9600 bps. This is to ensure that the extraction of the serial data is accurate and does not overlap with the next bit. The baud rate counter is made out of an incrementor and a comparator. The base value of the comparator is determined by equation (2):

$$Base\ Value = \frac{1}{Baud\ Rate \times 16} \times 50\ MHz \qquad (2)$$

The comparator will give a HIGH signal when the incrementor value is equal to the base value and a LOW when the value of the incrementor is less than the base value. The incrementor will increment by 1 at every clock cycle. When the incrementor hits the base value of the comparator, the value of the incrementor will be reset to 0 and the process repeats again.

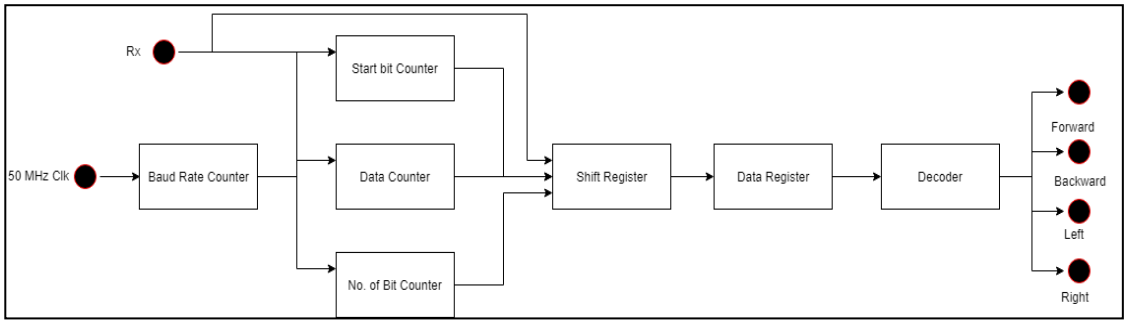

Fig. 5 - Block diagram of remote-control system

The information collected in the data register is decoded and a 4 bit output is generated. There are 8 recognised information by the decoder. For the recognised information, the respective output will give a HIGH signal whereas the others will remain as low. All four outputs will remain at LOW when any unrecognised information being stored. These information is shown in table 1.

Table 1 - Recognized information for decoder

Registered 8-bit Data	Movements
01000110	Forward
01000010	Backward
01001100	Left
01010010	Right
01000111	Forward + Left
01001001	Forward + Right
01001000	Backward + Left
01001010	Backward + Right
Any other info	Stationary

2.2 Sensor System

The sensor system consists of the Altera DE2-115 board and two HC-SR04 Ultrasonic Ranging module. The DE2-115 provides a trigger signal to the HC-SR04 module and receives an echo signal from the module. The DE2-115 board then analyses the duration of the echo signal and determine whether there is any obstacle at the front or at the back of the ALV and if a threat is present. The overall state diagram of the sensor system is shown in fig. 6.

Fig. 7 shows the block diagram of the sensor system. The sensor system consists of counters, a register, a comparator, and a multiplexer. The entire system is being clocked at a frequency of 50 MHz to ensure that there is no timing issues present within the sensor system. The system takes in one input from the ultrasonic ranging module, and provides two outputs, one for the ultrasonic ranging module and one for the propulsion system. As two ultrasonic sensors is being used, there are two sensor system providing obstacle detection at the front and the back respectively for the ALV.

The cycle reset counter is used to determine the end of a cycle. The cycle for the system is set at 50 ms. This is because any object that is present that can cause the echo pin to stay high for more than 50 ms does not pose a threat to the vehicle as it will be a distance away from the ALV and that allows the operator sufficient time to manoeuvre the vehicle away from the object. The base value of the trigger counter is determined by multiplying the frequency of the clock with 10 microsecond. The trigger output will be HIGH when the incrementor value is less than the base value. When the incrementor value reaches the base value, the incrementor holds its value and the trigger output is set to LOW. The counter then waits for the new cycle to arrive and then resets all the parameters and the cycle repeats itself. When echo feedback is detected, the echo pin will be set at HIGH. The distance counter will then start incrementing. When the incrementor reaches the base value of the comparator of the distance counter, which is the HIGH time of the width of the echo signal when the distance of the object is more than 50 cm away, the distance counter holds its value

and wait for the new cycle for all the parameter to be reset. If the distance counter has not achieved the base value of the comparator and the echo pin returns to a LOW, the value of the incrementor of the distance counter is transferred to a data register so that the value can be analyzed and decoded. The decoder of the sensor system is a comparator which compares the information stored in the data register with the base value, which is the HIGH time of the echo pin when the distance is at 20 cm. The decoder will give a HIGH signal when the value of the data register is lower than the base value of the comparator.

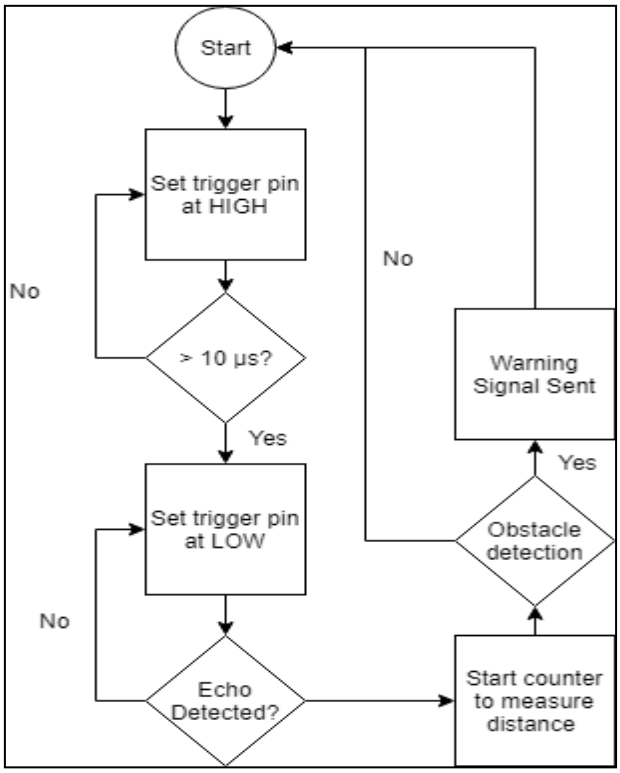

Fig. 6 - State diagram of sensor system

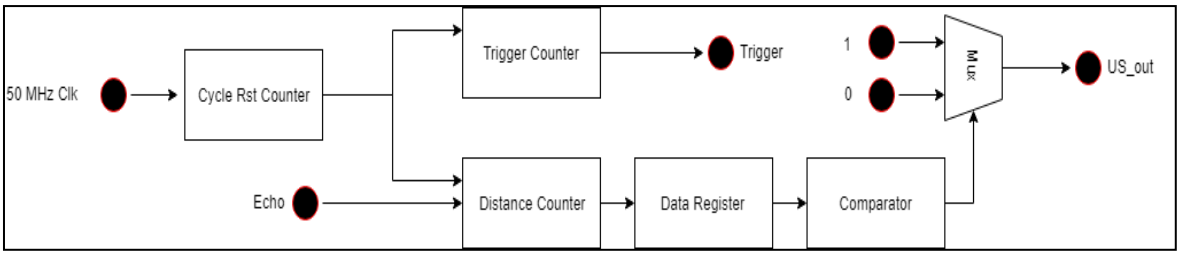

Fig. 7 - Block diagram of sensor system

The three systems were integrated and implemented on an Altera DE2-115 Board. All three design modules are integrated into a main project module and the inputs and outputs of the respective systems are wired together. The inputs of the overall system to the Altera DE2-115 board includes the Rx signal by the HC-06 Bluetooth module, and two echo inputs from two HC-SR04 Ultrasonic Ranging module. The clock is wired internally within the DE2-115 board. The overall system will then provide several outputs, two analogue outputs and two digital outputs to the motor driver, two trigger signals to the HC-SR04 Ultrasonic Ranging module, and two LED outputs to show the collision warning when an object is too near the ALV.

2.3 Mechanical Design of ALV

The ALV will be operating with three wheels present the vehicle. The vehicle moves with the two-wheel drive (2WD) concept, whereby two back wheels are receiving power from the power source (12 V LiPo batteries) simultaneously. The third wheel is positioned at the front of the vehicle where it provides support to the ALV by distributing the load and allowing smoother turning through freewheeling. Fig. 8 shows the mechanical design for the ALV, containing the top and bottom view, and the arrangement of all the electrical components. One LiPo battery is connected to the motor driver, which powers the motor driver and the two DC brushed motor. The second LiPo battery acts as the power source for the Altera DE2-115 Board. The Bluetooth module and the front ultrasonic ranging module is powered by the 5V pin of the motor driver whereas the back ultrasonic ranging module is powered by the 5V pin of the Altera DE2-115 board. There are four ground pins from the motor driver and 8 ground pins from the DE2-115 and all the ground pins are interconnected.

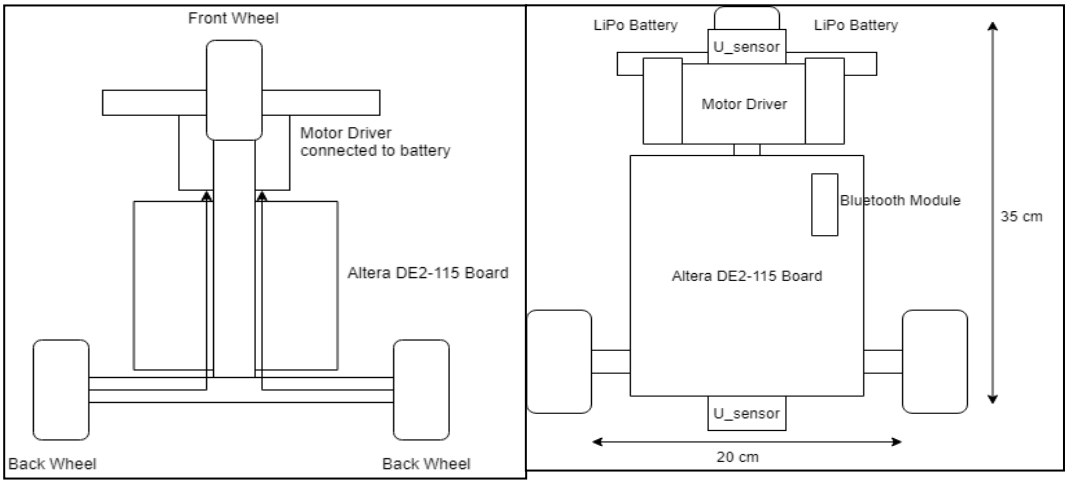

Fig. 8 - Top and bottom view of the vehicle

3. Results and Discussion

All three systems were designed and implemented on the prototype using Altera DE-115 FPGA board, SmartDriveDuo-30 DC brushed motor, HC-SR04 Ultrasonic Ranging Module, and HC-06 Bluetooth. Module Simulations on some of the system was performed using ModelSim-Altera 10.1d. Fig. 9 shows the prototype that was built.

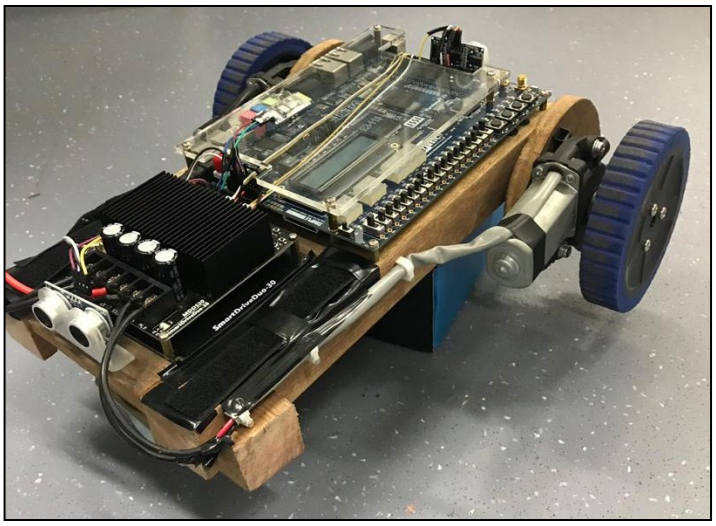

Fig. 9 - Prototype of the system

Fig. 10 shows the simulation when the operator instructs the ALV to move forward. This can be seen at point A in the figure. The analogue output for both the left motor and the right motor will generate a PWM signal with a duty cycle of 50%, indicating that both the DC brushed motor will rotate at 50% of the rated speed, hence pushing the ALV forward. The digital outputs for both motors are set at HIGH, indicating that the motor is rotating at a forward direction. These outputs can be seen at point B.

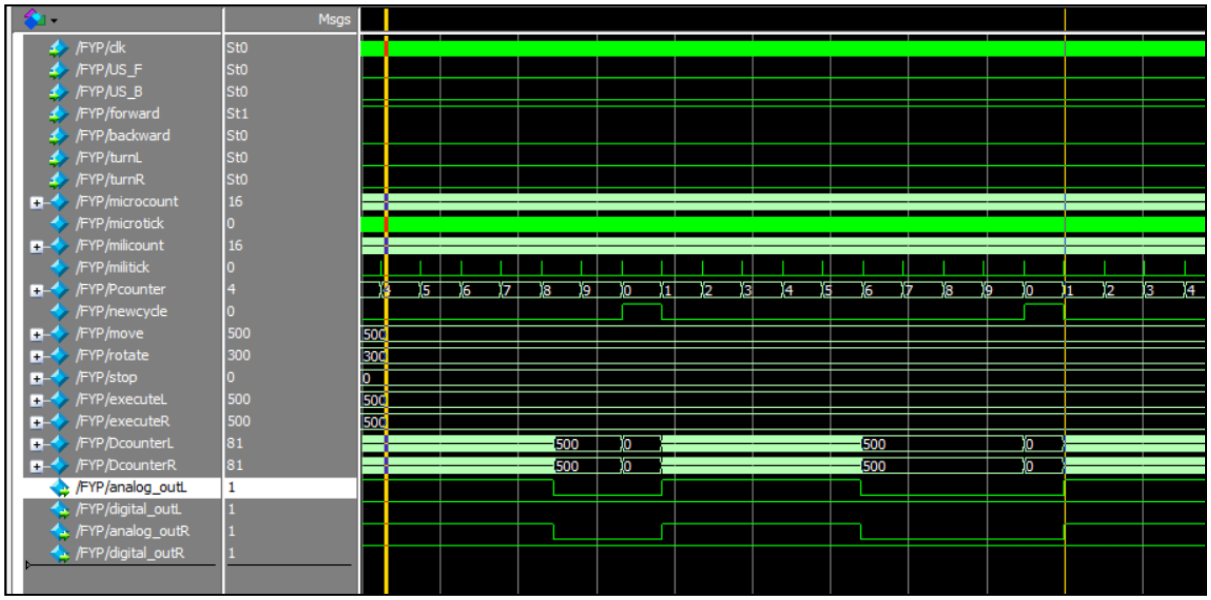

Fig. 10 - Waveform of propulsion system (forward)

When the input from the operator changes from “forward” to “backward” as shown at point A of fig. 11, the digital outputs for both the motors drop from HIGH to LOW, indicating that the rotational direction of the motor has changed from a forward rotation to a backward rotation. The analogue outputs of both the motors remains the same at a PWM signal with 50% duty cycle, indicating that the speed for both the motors remain the same. These can be seen at point B.

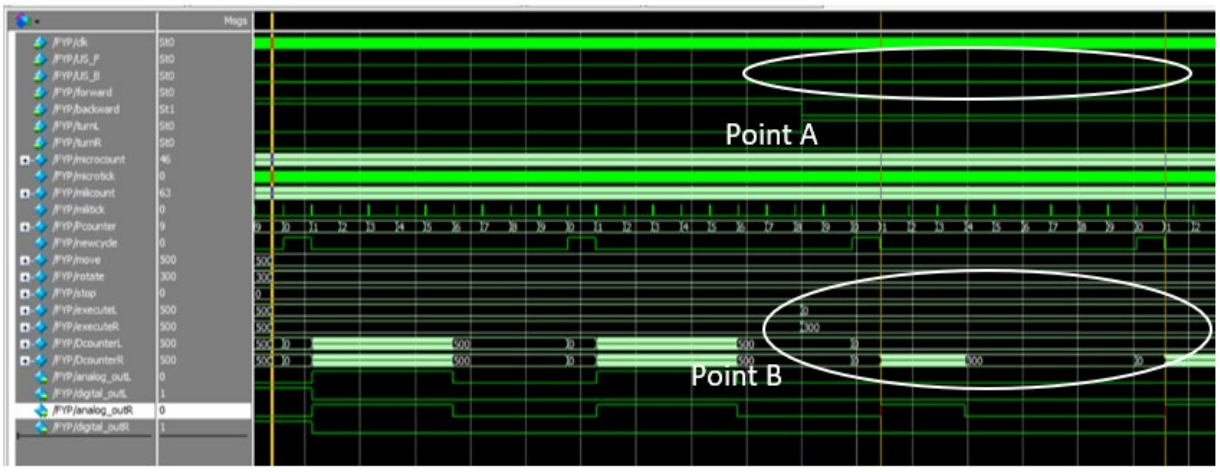

Fig. 11 - Waveform of propulsion system (backwards)

When the operator gives an input for the ALV to turn left, as seen at point A of Fig. 12, the duty cycle of the PWM signal for the left motor drops to 0% while the duty cycle of the PWM signal for the right motor drops to 30%. This can be seen at point B. This causes the left motor to stop rotating while the right motor rotates at a slower speed. This enables the vehicle to perform a stationary rotation towards the left.

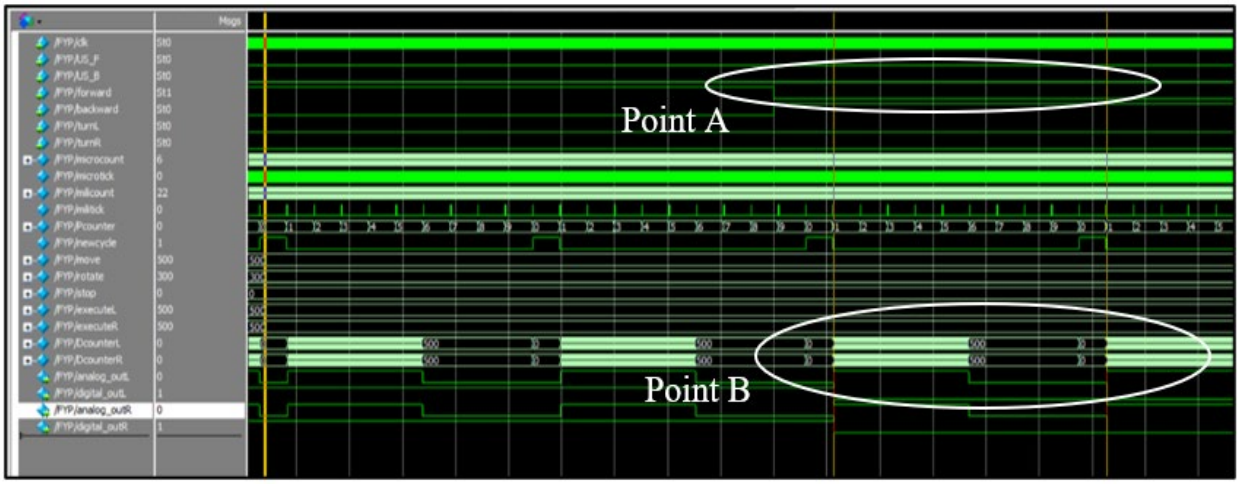

Fig. 12 - Waveform of propulsion system (left)

When the operator gives an input for the ALV to turn right, as seen at point A of fig. 13, the duty cycle of the PWM signal for the right motor drops to 0% while the duty cycle of the PWM signal for the left motor drops to 30%. This can be seen at point B. This causes the right motor to stop rotating while the left motor rotates at a slower speed. This enables the vehicle to perform a stationary rotation towards the right.

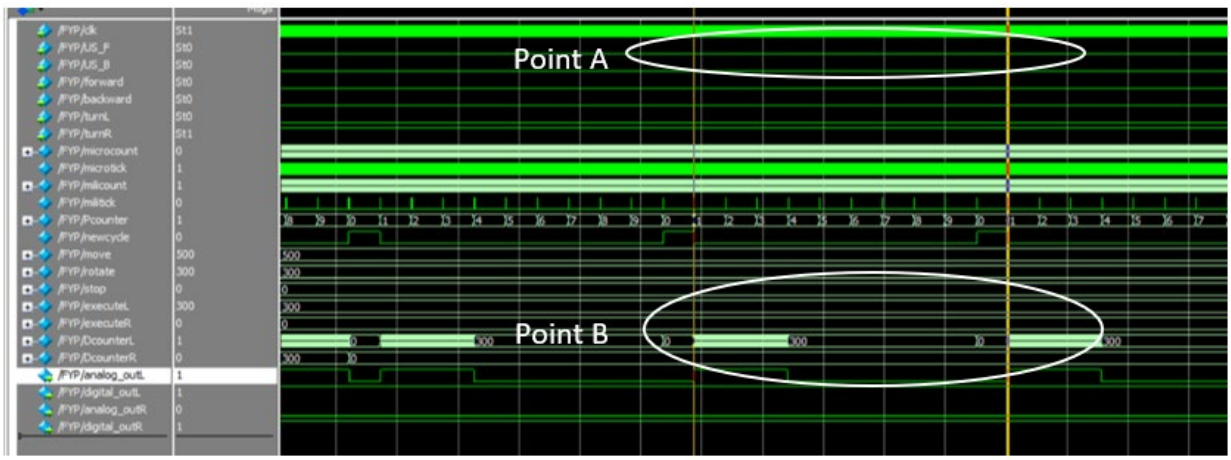

Fig. 13 - Waveform of propulsion system (right)

When the operator gives two inputs as shown at point A of fig. 14, instructing the vehicle to move forward and right at the same time, the PWM output for both the motors are slightly different. Looking at point B, it is shown that the duty cycle of the left motor is at 50% whereas the duty cycle of the right motor is at about 30%. The digital outputs of both motors are at HIGH, indicating that the motor is rotating at a forward direction. As both the motors are rotating, the ALV will move forward. On top of that, the left motor is rotating faster compared to the right motor, hence causing the vehicle to turn towards the right while moving forward.

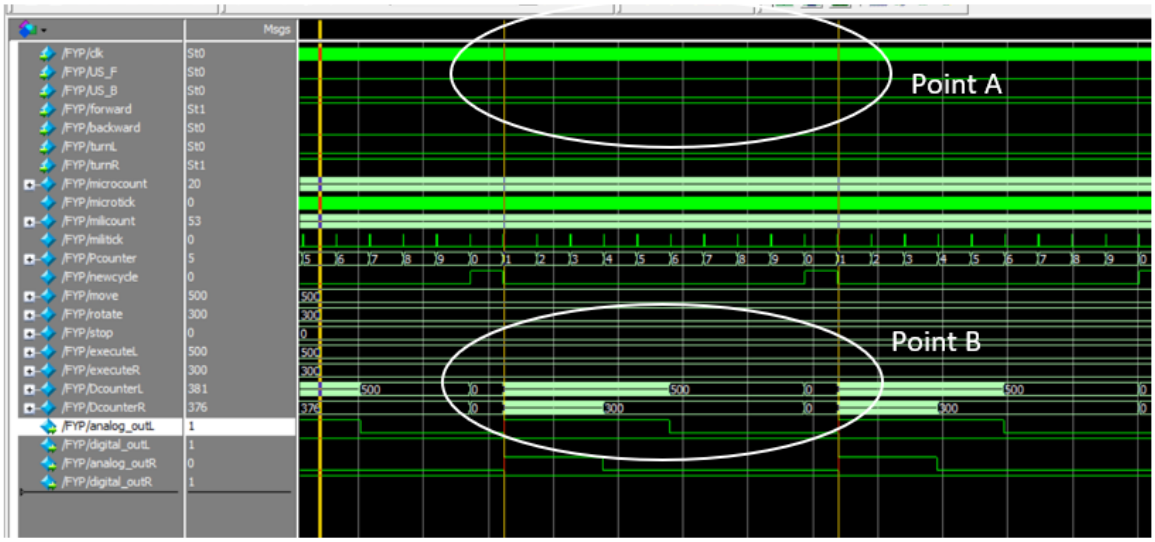

Fig. 14 - Waveform of propulsion system (forward and right)

When the operator changes the direction from forward to backward as shown at point A of Fig. 15, the PWM signal of both the outputs for the motors remains the same while the digital output for both the motors changes from HIGH to LOW, indicating a change in direction. These changes in the output can be seen at point B.

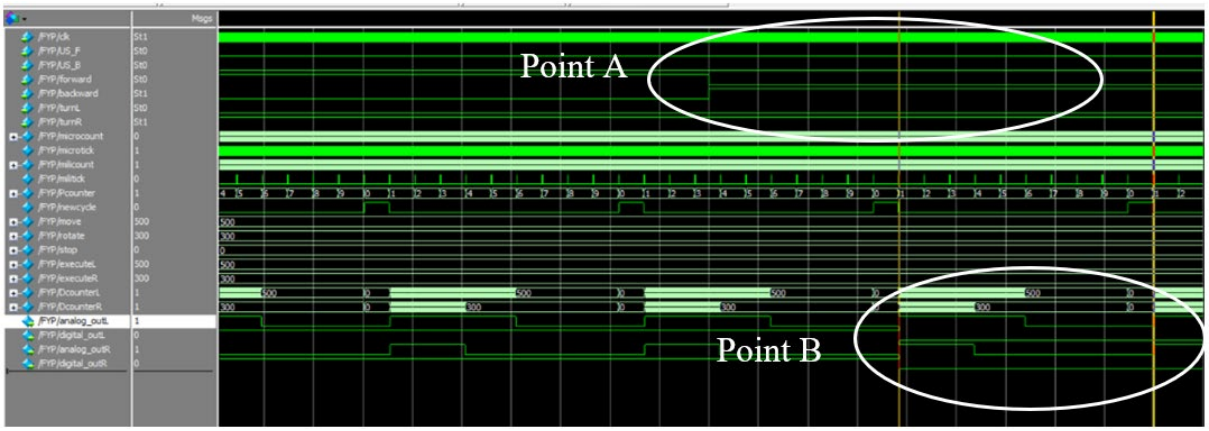

Fig. 15 - Waveform of propulsion system (backward and right)

Maintaining the movement of the ALV at backward right, an obstacle is now detected at the back of the vehicle as shown in point A of fig. 16. The vehicle immediately halts, by stopping the rotation of both motors. This can be seen at point B where the duty cycle of the PWM for both the left and the right motor dropped to 0%, indicating that the speed of the motors is now at 0.

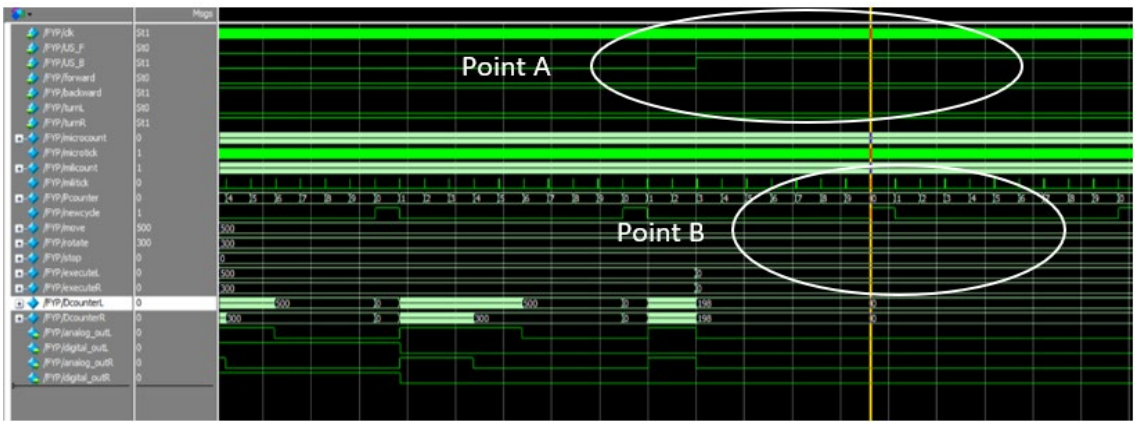

Fig. 16 - Waveform of propulsion system (obstacle detected)

Fig. 17 shows the waveform simulation when the operator of the ALV performs a corrective maneuver to bring the vehicle away from the obstacle. The operator changes the direction of the vehicle from moving backwards to forward. The system then allows the vehicle to perform the corrective maneuver instead of constantly halting the vehicle when an obstacle is detected. This can be seen at point B.

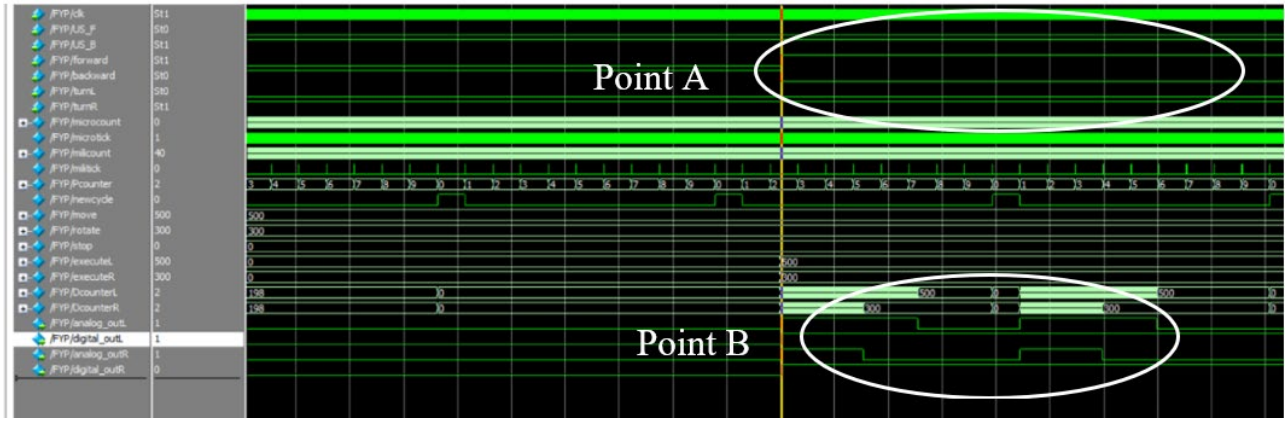

Fig. 17 - Waveform of propulsion system (corrective maneuver)

Fig. 18 shows the waveform of the remote-control system. When no data is received, the input remains at a HIGH state as shown at point A. When the start bit is detected at point B, the system starts to operate. The shift register then starts shifting to store the serial data that is being transmitted from the Bluetooth module. This can be seen at point C. When all 8 bits of data are shifted into the shift register, the information is then transferred to the data register to be decoded. The 4-bit output given out by the remote-control system is shown at point D.

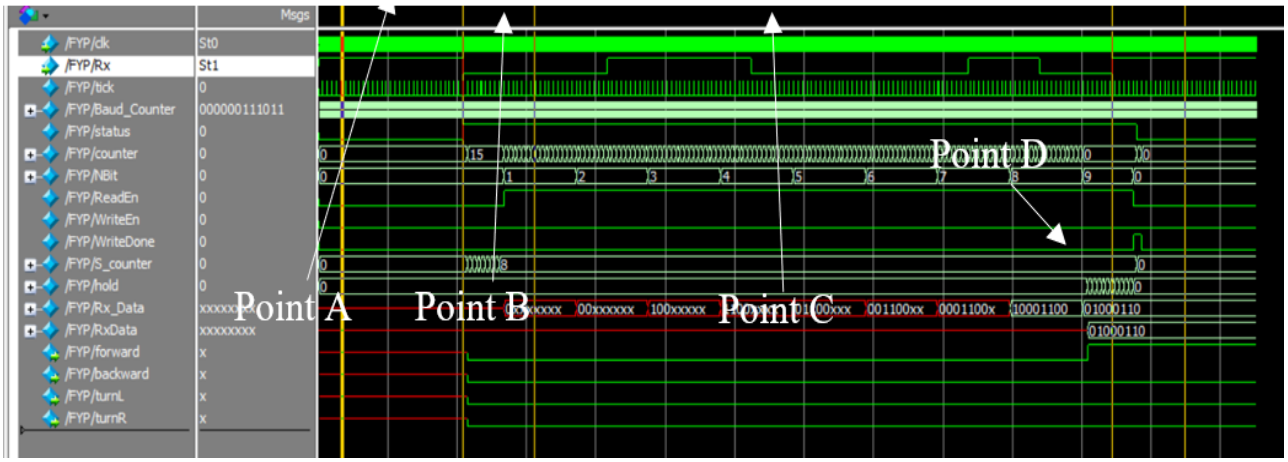

Fig. 18 - Waveform of remote-control system

In fig. 19, a test is conducted on the decoder when an unrecognized information is being received. At point A, the information received by the Bluetooth module is unrecognizable from the programmed information as shown in Table 1. The information is put through the decoder and the outputs are put to LOW, indicating that the vehicle will not move as the information given is unknown.

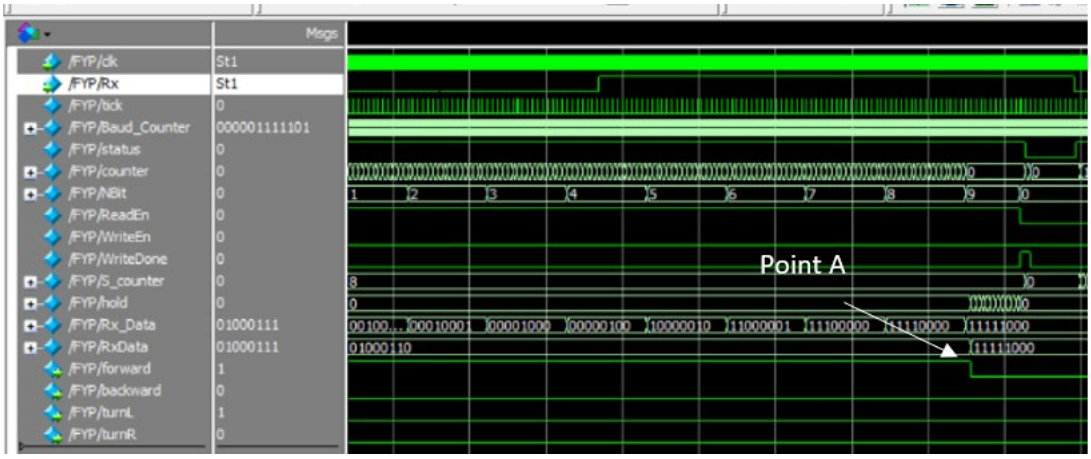

Fig. 19 - Waveform of remote-control system (unrecognized information)

In Fig. 20, a recognized information is now fed to the system. At point A, information that is being stored is now a recognizable information. The decoder then decodes the data, and sends the necessary output as shown at point A to the propulsion system according to table 1.

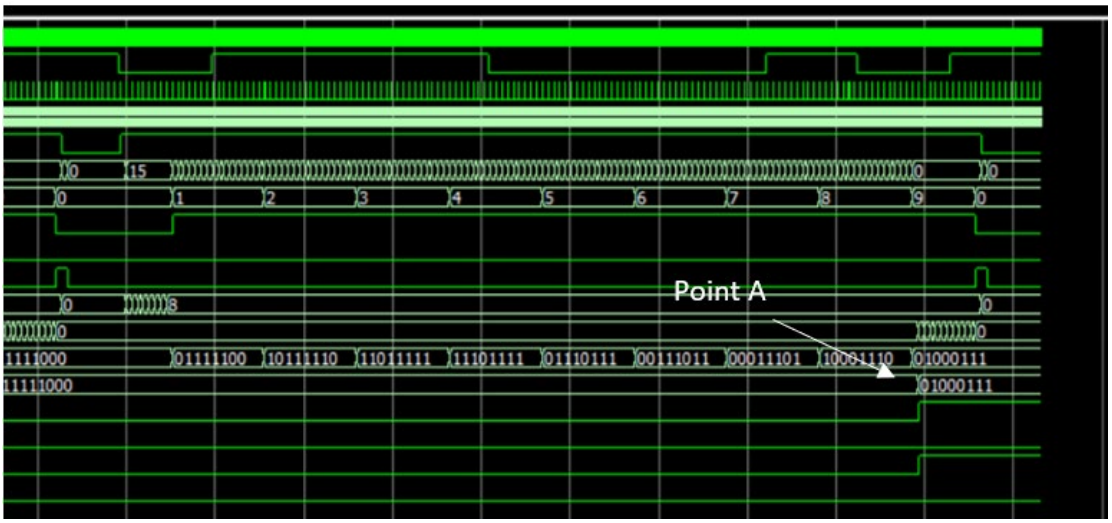

Fig. 20 - Waveform of remote-control system (recognized information)

Fig. 21 shows the application that is used as the remote of the ALV, sending serial data to the HC-06 Bluetooth module. The red button on the top left corner indicates that the device is not paired with the module. Once the module is paired up with the remote, the red button will turn green. For the prototype, only the arrow functions are being used.

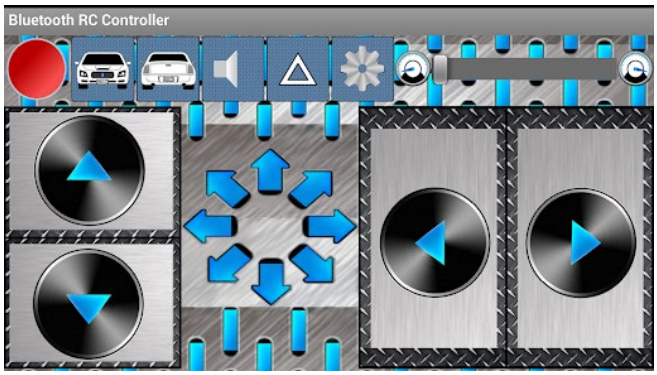

Fig. 21 - Remote-control for the ALV

Fig. 22 shows the results of the sensor system of the ALV. When an obstacle is detected in front and/or at the back of the vehicle, the vehicle goes to a halt position, and there will be an LED lighting up, indicating that an obstacle is

detected and is blocking the path of the vehicle. The LED is located at the Altera DE2-115 board below the in-built LCD screen.

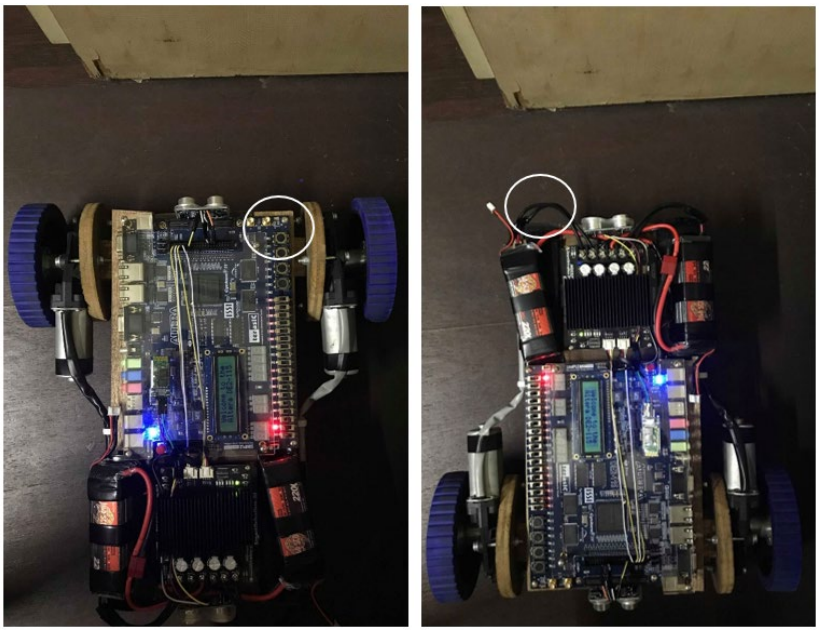

Fig. 22 - Prototype showing obstacle detection

Fig. 23 shows that an obstacle is detected at the back of the vehicle approximately 18 cm away. The collision warning is turn on, with the red LED light being on. Despite an obstacle being detected, the operator tries to move the vehicle backward, but the sensor system comes into play and restricts the vehicle to move nearer to the obstacle to prevent collision.

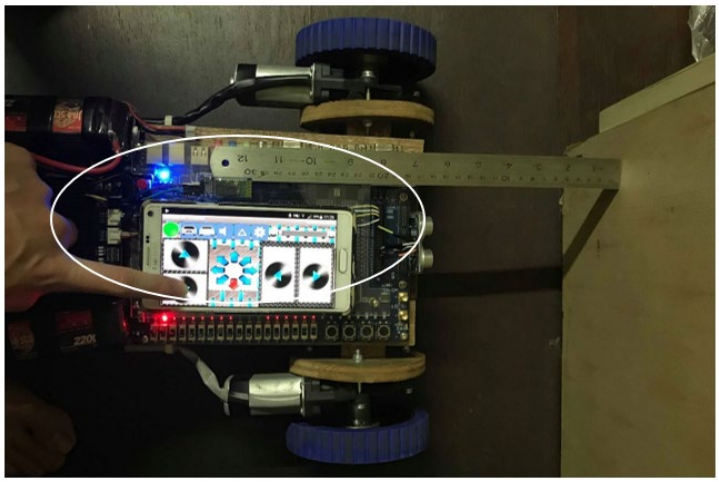

Fig. 23 - Sensor system

4. Conclusion

This paper proposed an FPGA to develop a compact real-time autonomous vehicle with a centralized controlling unit. The Altera DE2-115 was able to perform parallel processing, handling three systems at the same time with minimal time delay. The propulsion system, remote-control system, and the sensor system was also successfully designed. The DE2-115 was able to control a total of six electronics parts consisting of two DC brushed motor, one motor driver, two ultrasonic ranging modules, and a Bluetooth module. Lastly, a prototype of a compact real-time autonomous vehicle was also successfully created to proof that it is feasible to only have one FPGA unit as the central control unit for an ALV. Future work will consider using longer ranged and wider angled ultrasonic sensors, integrating a GPS tracker for a longer operational range for the ALV, and implementing some fuzzy algorithm to enable the vehicle to operate without the aid of the operator.

References

[1] Berns, K. and von Puttkamer, E. (2009) *Autonomous Land Vehicles*. Wiesbaden: Vieweg+Teubner. doi: 10.1007/978-3-8348-9334-5.

[2] Haustein, K. *et al.* (2017) 'A real-time Global Warming Index', *Scientific Reports*. Nature Publishing Group, 7(1), p. 15417. doi: 10.1038/s41598-017-14828-5.

[3] M.B.I. Reaz, F.Choong, M.S. Sulaiman, F. Mohd-Yasin (2007) *Prototyping of wavelet transform, artificial neural network and fuzzy logic for power quality disturbance classifier',* Electric power components and systems, 35(1), 1-17.

[4] YuHon Tee *et al.* (2010) 'A compact design of zero-radius steering autonomous amphibious vehicle with direct differential directional drive - UTAR-AAV', in *2010 IEEE Conference on Robotics, Automation and Mechatronics*. IEEE, pp. 176-181. doi: 10.1109/RAMECH.2010.5513192.

[5] KimChon Chan *et al.* (2010) 'Feasibility study of FPGA based Real-Time controller for autonomous vehicle applications', in *2010 IEEE Conference on Sustainable Utilization and Development in Engineering and Technology*. IEEE, pp. 1-6. doi: 10.1109/STUDENT.2010.5687010.

[6] De Castro, R., Araujo, R. E. and Oliveira, H. (2009) 'Design, development and characterisation of a FPGA platform for multi-motor electric vehicle control', in *2009 IEEE Vehicle Power and Propulsion Conference*. IEEE, pp. 145-152. doi: 10.1109/VPPC.2009.5289859.

[7] Afaq, A. *et al.* (2015) 'Development of FPGA-based system for control of an Unmanned Ground Vehicle with 5-DOF robotic arm', in *2015 15th International Conference on Control, Automation and Systems (ICCAS)*. IEEE, pp. 724-729. doi: 10.1109/ICCAS.2015.7365015.

[8] Chandra Kumar, R. *et al.* (2013) 'OBSTACLE AVOIDING ROBOT-A PROMISING ONE', *International Journal of Advanced Research in Electrical, Electronics and Instrumentation Engineering*, 2, pp. 2278-8875. Available at: www.ijareeie.com (Accessed: 19 April 2019).

[9] Ching-Heng Ku and Wen-Hsiang Tsai (2001) 'Obstacle avoidance in person following for vision-based autonomous land vehicle guidance using vehicle location estimation and quadratic pattern classifier', *IEEE Transactions on Industrial Electronics*, 48(1), pp. 205-215. doi: 10.1109/41.904581.

[10] Cui Huihai, Liu Shuqiang and Zeng Yingsheng (2011) 'An obstacle detection algorithm used sequential sonar data for Autonomous Land Vehicle', in *IEEE 2011 10th International Conference on Electronic Measurement & Instruments*. IEEE, pp. 255-259. doi: 10.1109/ICEMI.2011.6037990.

[11] Wu, T. *et al.* (2017) 'A feature matching and fusion-based positive obstacle detection algorithm for field autonomous land vehicles', *International Journal of Advanced Robotic Systems*, 14(2), p. 172988141769251. doi: 10.1177/1729881417692516.

[12] Xia, Y. *et al.* (2009) 'A Simple Obstacle Detection Approach Based on Stereo Vison in ALV System', in *2009 IITA International Conference on Control, Automation and Systems Engineering (case 2009)*. IEEE, pp. 395-398. doi: 10.1109/CASE.2009.47

[13] Karthikeyan, M., Sreeram, M. G. and Tech, M. (2014) 'Intelligent Exploration and Surveillance Robot In Defense Environment', *International Journal of Advanced Research in Electrical, Electronics and Instrumentation Engineering An ISO*, 3297(1). Available at: www.ijareeie.com (Accessed: 19 April 2019).